Tailoring the electronic structure and optical properties of cadmium-doped zinc oxides nanosheet

Saleem Ayaz Khan, Sikander Azam, Mohammed Benali Kanoun, Ghulam Murtaza, Malika Rani & Souraya Goumri-Said |

Published online: 27 Oct 2017.

Submit your article to this journal

Article views: 534

View related articles

View Crossmark data

Citing articles: 6 View citing articles

*Corresponding author: Souraya Goumri-Said, Department of Physics, College of Science, Alfaisal University, P.O. Box 50927, Riyadh 11533, Saudi Arabia
E-mail: sosaid@alfaisal.edu

MATERIALS SCIENCE | RESEARCH ARTICLE

Tailoring the electronic structure and optical properties of cadmium-doped zinc oxides nanosheet

Saleem Ayaz Khan[1], Sikander Azam[2], Mohammed Benali Kanoun[3], Ghulam Murtaza[4], Malika Rani[5] and Souraya Goumri-Said[3]*

Abstract: Cd-doped ZnO nanosheet (ZnO NS) were investigated using a full-potential linearized augmented plane wave method within the generalized gradient approximation (GGA) to calculate the electronic structure and its optical response. The calculated band structures have shown that the Cd-doped ZnO NS is a direct band gap semiconductor at Γ with 1.50 eV band gap. The contribution of each atom/orbital were commented in light of total and partial densities of states. We also derived the optical constants (mainly the dielectric constants $\varepsilon_1(0)$ and $\varepsilon_2(0)$), the absorption coefficient $I(\omega)$, refractive index $n(\omega)$, extinction coefficient $k(\omega)$, and energy-loss function $L(\omega)$. The spectrum of absorption coefficient has revealed to increase rapidly for photon energies higher than 2.5 eV. The absorption spectrum was found to be limited in energy region due to different contributions electronic transitions that occurred within ZnO NS and effect of Cd doping. Reducing the band gap of ZnO NS to low values is suitable process for light-emitting devices and solar cells applications.

Subjects: Chemistry; Material Science; Metals & Alloys

Keywords: ZnO nanosheet; solar cells; DFT; optical properties; electronic structure

1. Introduction

A monolayer layer of carbon atoms in honeycomb structure, graphene, is offering exceptional properties (Avouris, Chen, & Perebeinos, 2007; Geim & Novoselov, 2007; Katsnelson, Novoselov, & Geim, 2006) that have led to important applications in various fields, such as spintronics, (Novoselov et al.,

ABOUT THE AUTHORS

This work was achieved by the computational material science group (S. Goumri-Said and M. B. Kanoun) of Physics Department at Alfaisal University (Saudi Arabia) and the researchers from Lahore University (S. Azam) and the University of West Bohemia (S. A. Khan). All researchers have collaborated since 2015 and published joint works using the recent computational theories (density functional theory and the recent approaches of the exchange and correlation term). The present authors have studied different materials such as: chalcogenides and selenides for various applications: magnetism/spintronics, optoelectronic, thermo-electric, and photovoltaic. Recently, the team has extended their interest to new forms of materials: the layered, thin-films, and 2D systems.

PUBLIC INTEREST STATEMENT

Graphene and 2D materials in general, have revolutionized our way to perform research and innovate for the benefit of industry and society. They have shown advantageous properties such as flexibility and lightweight. In the future, 2D materials will enable particular innovation of new electronic circuits, due to their exceptional conductive properties. ZnO in 2D or ZnO nanosheet has shown the possibility to tune its electronic and optical properties by an appropriate doping with transition metal. The huge band gap of the ZnO was reduced. In general, 2D materials have shown the ability to tune their physical properties by doping or creation of vacancies.

2005) optoelectronic (Ma, Yan, Xiao, & Chen, 2010), and energy (Ouyang, Peng, Liu, & Liu, 2011). Whereas, graphene was found semi-metallic and its electrons and holes behave like a massless Dirac fermion. Two-dimensional (2D) boron nitride (BN) (Lin & Connell, 2012) Group III–V is graphene-like sheets form were found to be a wide band gap semiconductors. Further, it has been realized that other III–V compounds can stabilized also in 2D monolayer honeycomb structures, such as ZnO and its nanowires that have shown the possibility of graphitic ZnO growth (Claeyssens, 2005; Kulkarni, Zhou, Sarasamak, & Limpijumnong, 2006; Wang, Fan, & Sun, 2009). In fact, zinc oxide (ZnO) materials have attracted extensive attention for half a century because of their excellent performance in different areas such as optoletronics, photoelectronics, catalytic (Al-Sunaidi & Goumri-Said, 2011; Duan, Huang, & Wang, 2005; Huang et al., 2006; Khan, Azam, Shah, & Amin, 2015; Wang, Sun, Chen, Kawazoe, & Jena, 2008) and, most recently, spintronics (Bantounas et al., 2011).

ZnO has a wide band gap of 3.3 eV and large exciton binding energy of 60 meV that has led to various optoelectronic applications such as light-emitting diodes and photovoltaic (PV) devices (Hwang, Oh, Lim, & Park, 2007; Law, Greene, Johnson, Saykally, & Yang, 2005; Ul Haq, Ahmed, & Goumri-Said, 2014). Recently, vacancy defects have been introduced intentionally ZnO in order to tune its optoelectronic response using the electron irradiation technique. Similarly to the honeycomb graphene, the vacancies have induced ferromagnetism as well as the doping using transition metal atoms (Bantounas et al., 2011; Kanoun, Goumri-Said, Manchon, & Schwingenschlögl, 2015). The enhancement of magnetic properties using dopants and defect might be useful for biomedical applications (drug delivery) as ZnO has nontoxic nature that can compensate the metal ions toxicity.

A recent study based on sol–gel method has improved the photoluminescence properties and performance of Cd-doped ZnO in quantum dots (QDs) (Zhang, Zhao, Zhang, Zhou, & Cai, 2012). Cd dopant concentration has changed the structural and luminescent properties of ZnO-QDs. It was observed that when the Cd concentration was increased, the QD particle size was reduced; leading to a significant of fluorescence intensity activity. In similar way, using a one-step, wet-chemical synthesis technique, it was possible to obtain a polycrystalline ZnO NS with potential use in a blue-white fluorescent coating for UV sources (Vempati, Mitra, & Dawson, 2012).

In the present work, a comprehensive study was conducted to understand the relationship between the electronic structure and the optical response of cadmium-doped ZnO in nanosheet form. We used the state of art of density functional theory (DFT) to explore the electronic band structure, density of states, and related optical properties. These properties have leaded us to broaden our knowledge about tailoring the optoelectronic properties of Cd-doped ZnO NS for potential use in LEDs and PV applications as the Cd has trend to reduce drastically the ZnO band gap.

2. Computational detail

In the present computational work, we considered the stable structure for pure ZnO crystal: wurtzite. It consists of Zn and O plane stacked alternatively along c-axis. We constructed the ZnO NS supercell from the optimized bulk ZnO with lattice parameters a = 3.29 Å, c = 5.3 Å (Kanoun et al., 2015). The 2D ZnO NS modeled by cutting from bulk ZnO (0001) plane, as shown in Figure 1, containing 30 formula units. We used a vacuum region of 15 Å to the (0001) plane to avoid artificial interactions between two layers. To this aim, we replace one Zn atom in this supercell by Cd, which gives rise to a doping level of 6.67%.

Figure 1. Structures of ZnO nanosheet and Cd-doped ZnO nanosheet used in computational works.
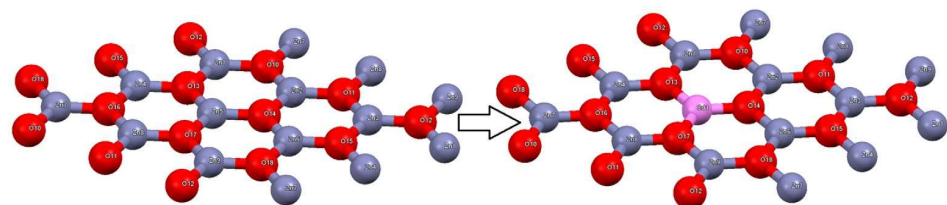
The computations were performed using the first principle full-potential linear augmented plane wave (FP-LAPW) method, as implemented in WIEN2 K code (Blaha, Schwarz, Madsen, Kvasnicka, & Luitz, 2008), based on the generalized gradient approximation (GGA) (Hohenberg & Kohn, 1964; Perdew, Burke, & Ernzerhof, 1996) for the exchange–correlation potential within the framework of density functional theory (DFT) (Delin, Ravindran, Eriksson, & Wills, 1998). The wave function, charge density, and potential were expanded in spherical harmonic functions inside the non-overlapping muffin tin (MT) spheres and among Fourier series in the interstitial region. The plane waves cut-off parameter was KMAX × RMT = 7.0, in order to achieve the convergence for energy eigenvalues. Atomic sphere radii of Zn/Cd, and O atoms are set to 1.89, and 1.63 a.u., respectively. The orbitals of Zn (3d10 4s2), Cd (4d10 5s2), and O (2s2 2p4) were treated as valence electrons, while the lower states are deal as a core states. The self-consistent potentials were performed on a 7 × 7 × 1 k-mesh in the Brillouin zone. The Brillouin zone (BZ) is represented by the set of 7 × 7 × 1 k-points (Kittel, 1996) for our calculations. The structural relaxation is done until the forces on each atom are smaller than 0.0001 meV Å^{-1}.

The dielectric function $\varepsilon(\omega) = \varepsilon_1(\omega) + \varepsilon_2(\omega)$ has a direct relation with the band structure of materials. It (dielectric function) is considered as a key for the calculation of the optical response of the solid materials to electromagnetic interference. In principle the dielectric function, should consist of intra- and inter-band transitions. But, the intra-band transition is limited to metals. The inter-band transitions have split into direct and indirect band transitions. Here, in our calculations, the phonon contribution is ignored and the direct transition zone between the occupied (valence) and unoccupied (conduction) states is considered. The imaginary part of dielectric function $\varepsilon_2(\omega)$ (Penn, 1960) can be calculated using the following expression:

$$\varepsilon_2^{ij} = \frac{4\pi^2 e^2}{Vm^2\omega^2} \times \sum_{nn'\sigma} \left\langle kn\sigma \left| p_i \right| kn'\sigma \right\rangle \left\langle kn'\sigma \left| p_j \right| kn\sigma \right\rangle \times f_{kn}\left(1 - f_{kn'}\right)\delta\left(E_{kn'} - E_{kn} - \hbar\omega\right) \tag{1}$$

where m and e are the mass and charge of the electron, whereas ω is the frequency of the incident photons on the crystal. V is volume of unit cell. The $|kn\sigma\rangle$ represents the crystal wave function with k being the crystal momentum and σ spin. Fermi distribution function f_{kn}, counts transition between the occupied and unoccupied states. The electric dipole transitions between valence and conduction band give rise to the peaks in the optical response.

The real part $\varepsilon_1(\omega)$ is calculated from imaginary part using Kramers–Kronig relation (Penn, 1960):

$$\varepsilon_1(\omega) = 1 + \frac{2}{\pi}P\int_0^\infty \frac{\omega'\varepsilon_2(\omega')}{\omega'^2 - \omega^2}d\omega' \tag{2}$$

where p is the principle value of integral.

Besides, for obtaining exact optical absorption spectra in low energy range, the scissors correction (Fiorentini & Baldereschi, 1995) has been carried out in optical absorption of pure and Cd-doped ZnO NS using the calculated band gap with from the present DFT electronic structure.

3. Results and discussion
To illustrate the electronic structure, we have calculated the band structure of the pure and Cd-doped ZnO NS, as displayed in Figure 2. Our results show that both systems have direct band gaps. The nature of the direct band gap semiconductor is observed at the Γ-symmetry point. The calculated direct band gap value for pure ZnO NS is 1.70 eV. While replacing Zn by Cd pull the conduction band down toward the Fermi level (EF) that decreases the energy band gap value to 1.50 eV, as shown in Table 1. Further elucidating the nature of the electronic structure, the total and partial density of states (TDOS and PDOS) for Cd-doped ZnO NS have been calculated, as shown in Figure 3. The total density of states (TDOS) of pure and Cd-doped ZnO NS, see Figure 1(a), and shows a similar behavior except that doping ZnO NS by Cd, the minimum conduction band moves toward lower

cogent · physics

Figure 2. Band structures of ZnO nanosheet and Cd-doped ZnO nanosheet.
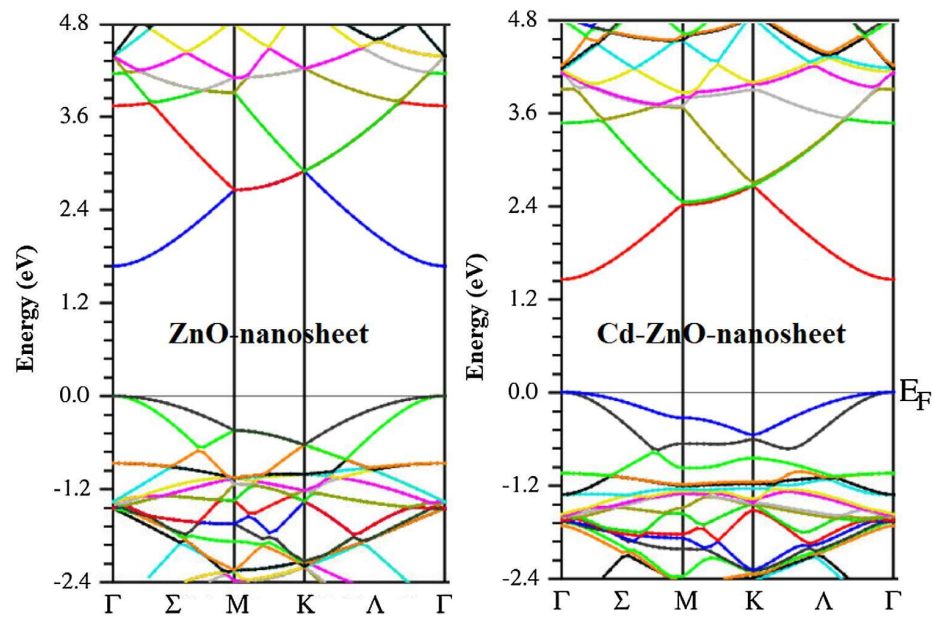
Table 1. Calculated band gap, static value of the birefringence and effective masses as calculated for ZnO NS and Cd-doped ZnO NS systems

	ZnO	Cd/ZnO
E_g(eV)	1.695*, 3.29–3.32ᵃ	1.4990*
$\delta\varepsilon$	−0.1086*	−0.1159*
$\Delta n(0)$	−0.1345*	−0.1446*
m_e^*/m_e	0.0107*	0.0336*
m_{hh}^*/m_e	0.0932*	0.0941*
m_{lh}^*/m_e	0.0483*	0.0329*

*Present work.

ᵃExperimental work (Zhang et al., 2012).

energies. In Figure 3(b), we represented Zn/Cd 3d/4d and O 2p states. It appears that the valence band maximum (VBM) mainly comprises Zn/Cd d and O p states hybridizations, where the Cd d and O p states show strong hybridization than Zn d and O p states. The Zn/Cd d and anion O p states show greater contribution in the region between −3.0 and −1.0 eV. Whereas, it shows the lowest contribution in the upper valence band, i.e. the region between −4.0 and −3.0 eV. In addition, the lowest conduction band is mainly comprises O p states. Thus, the band gap is shaped among the occupied and unoccupied of Zn/Cd d states and O p unoccupied states. Analyzing the DOS, we found that the O p anti-bonding interaction modifies the band gap value for Cd-doped ZnO NS. Moreover, Figure 3(c) shows that Cd d states hybridized strongly with O p states in comparison with Zn d states. This reflects that the bonding (covalent) between Cd–O will be stronger than Zn–O.

In order to better assess the bonding interaction within the NS, we have calculated the valence electronic charge density (ECD) of pure and Cd-doped ZnO NS along the (001) crystallographic plane, as illustrated in Figure 4. A significant covalent bonding character exists between Zn/Cd and O atoms owing to the sharing of charge between them. Moreover, we show that there is charge transfer from Zn and Cd atoms toward O atom. These charge rearrangements reflect the Pauling electronegative nature of O where the Zn (Cd) and O have 1.6 (1.69) and 3.44 electronegativity. Furthermore, the

Figure 3. (a) Total DOS of ZnO nanosheet and Cd-doped ZnO nanosheet. **(b)** Partial DOS for ZnO nanosheet. **(c)** Partial DOS for Cd-doped ZnO nanosheet.
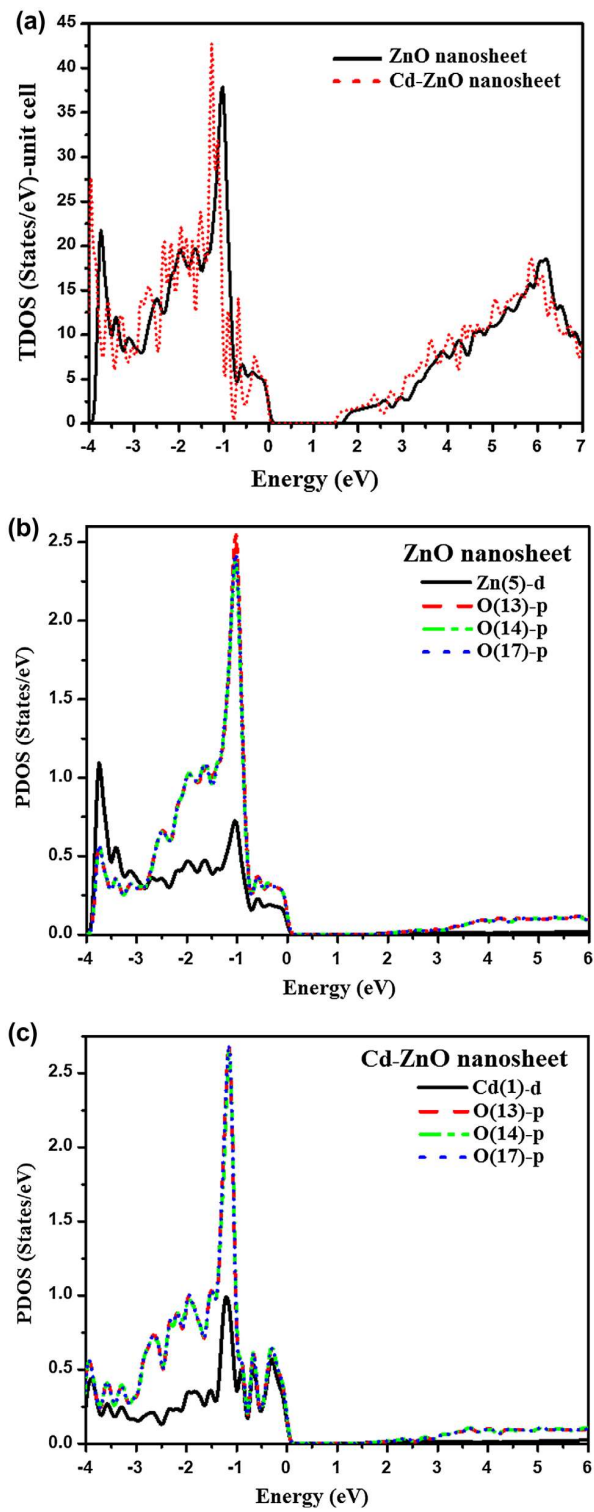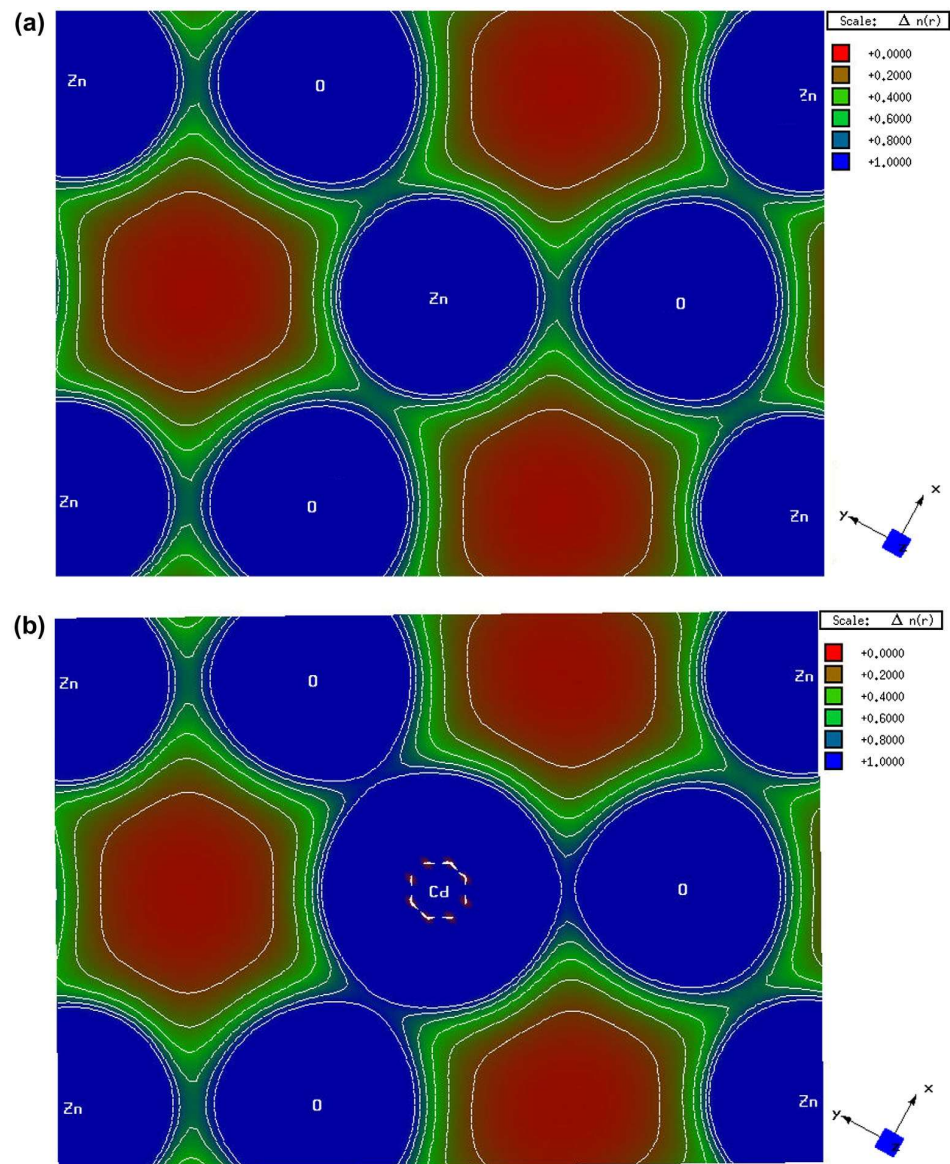
cogent ·· physics

Figure 4. Charge densities of (a) pure and (b) Cd-doped ZnO.

covalent bonding became stronger when Zn replaced by Cd. This is due to strong hybridization between Cd and O.

The optical properties of Cd-doped ZnO NS can be illustrated using the complex symmetric tensor of dielectric function ($\varepsilon(\omega)$). Our investigated systems have a hexagonal symmetry that has two independent components, that corresponds to the electric field E, directed along a and b crystallographic axes. The average real part of the dielectric functions pure and Cd-doped ZnO NS have been calculated, and displayed in Figure 5(a). The real part of the spectra allows us to find out the static dielectric constant, $\varepsilon_1(0)$ values. As we can see in Figure 5(a), the static value of the dielectric constant shifts up when Zn was substituted by Cd, this is due to the energy gap (E_g) change. The relation between $\varepsilon_1(0)$ and E_g can be enlightened on the basis of Penn Model (Kanoun et al., 2015), $\varepsilon_0 = 1 + \left(\hbar\omega_p / E_g \right)^2$, reflecting the inverse relation between the dielectric constant and the band gap energy. The $\varepsilon_1(0)$ contingent on the polarization directions which display an optical anisotropy

Figure 5. Comparison of dielectric responses : (a) dielectric constant, ε_1, of ZnO nanosheet and Cd-doped ZnO nanosheet, (b) dielectric constant, ε_2, of ZnO nanosheet and Cd-doped ZnO nanosheet, (c) dielectric constant, ε_2 vs. wavelength to show the peaks shift toward the higher energies.
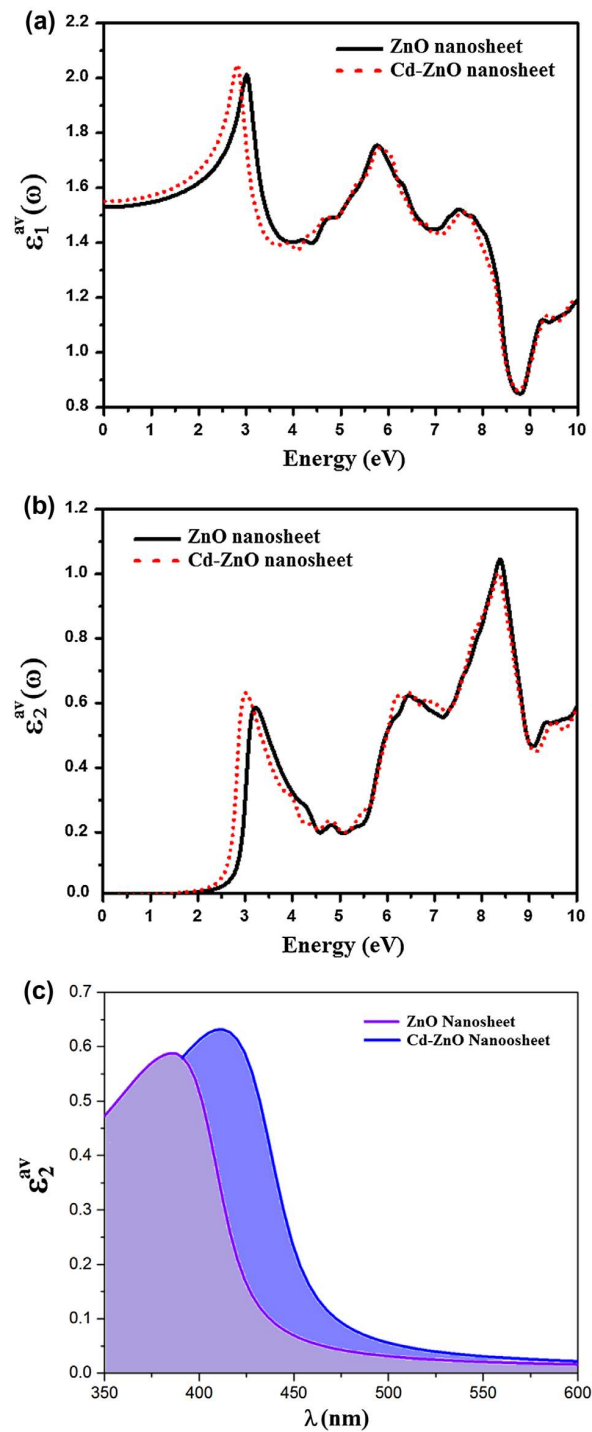
that can affect other related optical properties derived from the dielectric function. In the present work, we only considered the average of the polarization direction. As already mentioned, the symmetry of the considered systems leaded us to consider two major non-zero components from which the uniaxial anisotropy was obtained using the formula: $\left(\delta\varepsilon = \left[(\varepsilon_0^{zz} - \varepsilon_0^{xx})/\varepsilon_0^{tot} \right] \right)$. $\delta\varepsilon$ was estimated about −0.152 and −0.167 for pure and Cd-doped ZnO NS systems, respectively. This confirms the

existence of the anisotropy. Taking in account the partial densities of states, we have calculated the imaginary part in order to obtain the energy levels. Rendering to the dipolar selection rule only transitions whose angular momentum quantum number changes by unity ($\Delta = \pm 1$) are allowed.

Figure 5(b) gives the imaginary part of dielectric function of pure ZnO NS which shows three major peaks. The first peak is mainly composed of the optical transitions between O 2p states (in the highest valence band) to Zn 4s states (in the lowest conduction band). The second and third peaks are due to optical transition between the Zn 3d and O 2p states. Following the substitution of Cd, we observed a small shift of the main peaks of Cd-doped ZnO NS toward lower energy (Figure 5(b)). Moreover, the shift of the optical transition indicates that the direct band gap is decreasing, which is in good agreement with the result of DOS. The calculated average imaginary part of dielectric function versus wavelength in Figure 5(c) shows that the peaks shift toward the higher energies and the optical response of the Cd-doped ZnO NS shifted from violet to blue region.

All the related optical constants can be derived from ε_1 and ε_2, such as absorption coefficient $I(\omega)$, refractive index $n(\omega)$, extinction coefficient $k(\omega)$, and energy-loss function $L(\omega)$. Our results indicate that the spectrum of absorption coefficient $I(\omega)$ has increased rapidly for photon energies higher than 2.5 eV, as shown in Figure 6(a). From the last figure, the strong absorption extends in the region between 2.5–10.0 eV. $I(\omega)$ spectrum in the limited energy region exhibits different peaks that are caused by different electronic transitions. The width of the absorption is contingent on the band gap of a material. The peaks variation in the absorption spectrum shows that the investigated compounds have potential application for optoelectronic devices. Hence, the $I(\omega)$ spectrum shows threshold energies occurring at 2.7 and 2.5 eV in the pure and Cd-doped ZnO NS. These values are related to band edge absorption. Away from the threshold, the $I(\omega)$ increase speedily as a result of the strong band edge absorption, the region where we have strong absorption is interesting to explore for potential use in PV devices. For both systems (pure and doped), the curves of the absorption coefficient plots are showing no significant difference.

The calculated refractive index spectra for the Cd-doped ZnO are plotted in Figure 6(b). It is obvious that at low energies the refractive index shows an inverse relation to the width of the band gap. It is well known that the wider band gap semi-conducting materials have the lower refractive index which undergoes an inverse relation between the zero frequency limit of the refractive index and band gap of semiconductor. From Figure 6(b), we might observe that $n(\omega)$ increases with energy in transparent region reaching a peak around 2.0–4.0 eV. Beyond this limit, the refractive index drops sharply. At low frequency ($\omega = 0$), the square root of $\varepsilon_1(0)$ can be used to estimate the refractive index calculated as −0.135 and −0.145 for pure and Cd-doped ZnO NS, respectively. The maximum peak of the $n(\omega)$ appeared at 3.0 eV. Beyond this energy range, a decrease occurred with increasing energies as well as several small peaks appeared at specific energies. The refractive index follows the pattern of the real part of the dielectric function. The refractive index is a significant physical parameter that is connected to the microscopic atomic interactions. Theoretically, $n(\omega)$ is inter-related to the local polarizability as well as the electronic density of the investigated compound. The birefringence is essential merely in the non-absorbing region, which is beneath the energy gap. The $\Delta n(\omega)$ spectral reliance displays a strong oscillation in the energy range from 1.5 to 7.0 eV. The static value of the birefringence $\Delta n(0)$ is listed in Table 1 for pure ZnO NS and Cd-doped ZnO NS systems.

The calculated extinction coefficient $k(\omega)$ is presented in Figure 6(c). It shows the same behavior as $\varepsilon_2(\omega)$. The local maxima are found at 3.0, 7.0, and 8.5 eV for both systems. It is obvious from Figure 5(a) that $\varepsilon_1(\omega)$ shows lower values at these energies point. The broad edge (i.e. from 0.0 to 2.5 (2.3)) of the absorption spectra which indicate that the Cd-doped ZnO NS is transparent in this energy region and can be used as transparent semiconductor for a new fangled generation of optoelectronic devices.

The energy loss function spectra represent the characteristic associated to plasma resonance and might be used to illustrate macro- and microscopic properties of solid materials. The energy-loss

Figure 6. Comparison of the related optical properties between pure ZnO NS and Cd-doped ZnO NS : (a) absorption coefficient $I(\omega)$, (b) refractive index $n(\omega)$, (c) extinction coefficient $k(\omega)$, (d) energy-loss function $L(\omega)$, and (e) reflectivity spectra $R(\omega)$.

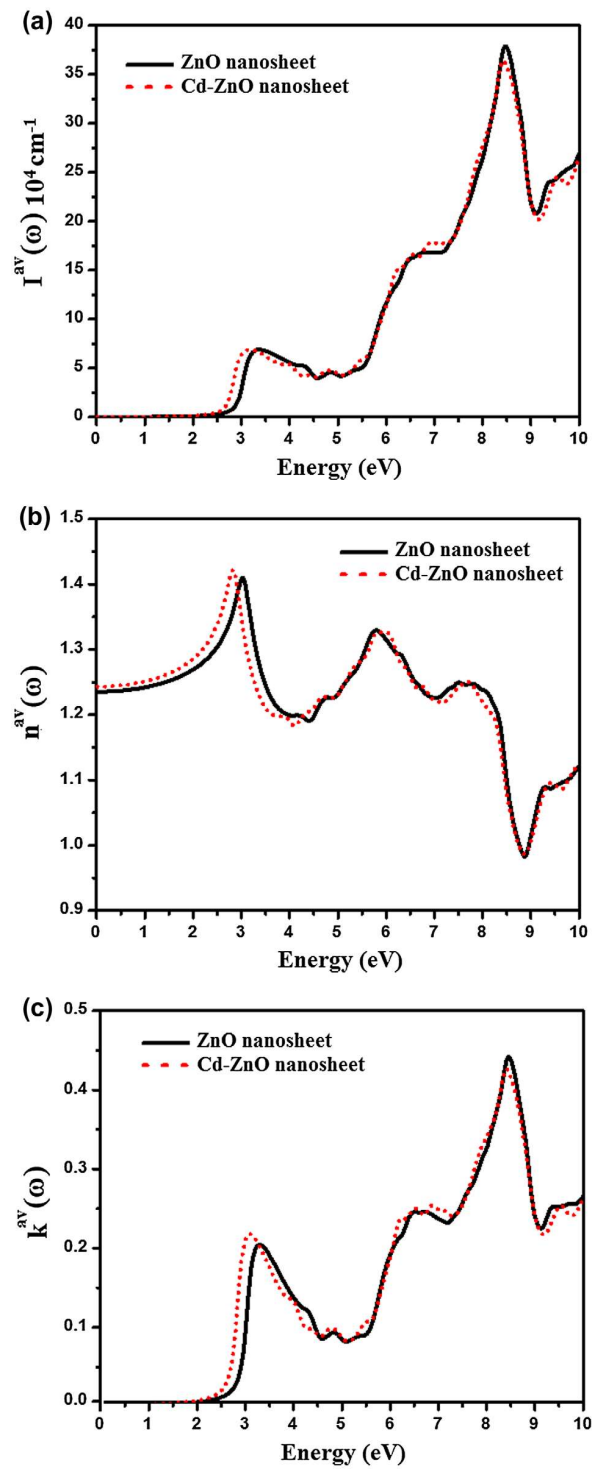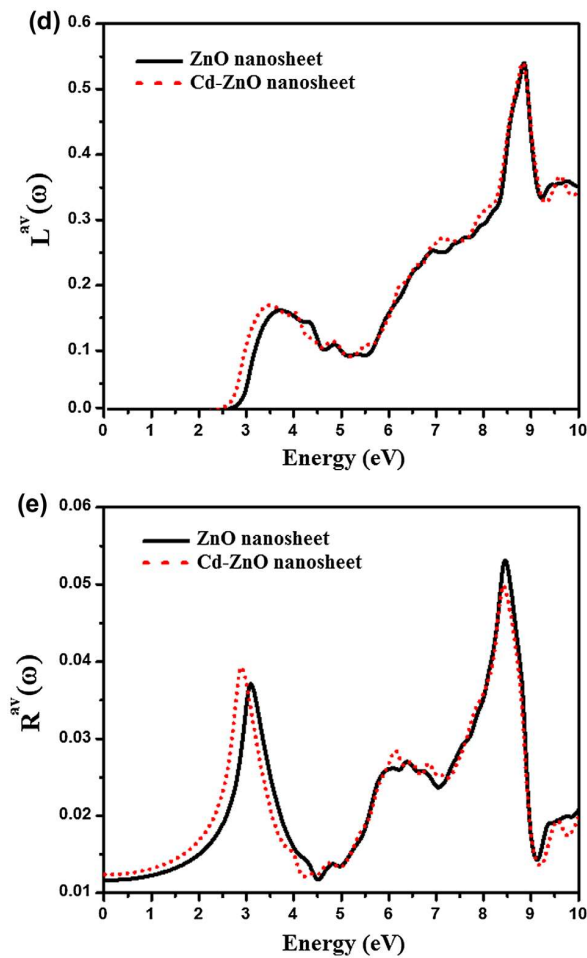**Figure 6. (*Continued*).**

(d)

(e)

function shows a direct relation with the probability of a fast moving electron across a material loses energy per unit length, as displayed in Figure 6(d). In the energy loss function spectra, the prominent peaks are known as a plasmon peak, indicating the energy of collective excitations of the electronic charge density in the material. The maximum peaks are located at 3.5, 7.0, and at 9.0 eV for both systems. Finally, in Figure 6(e), we provide the reflectivity spectra for pure and Cd-doped ZnO NS. These plots are exhibiting sharp peaks at 3.0, 6.0 and at 8.3 eV for both systems. These maximum peaks are raised from inter-band transitions. Furthermore, in the reflectivity spectra, we observe a rapid reduction at ≈9.2 eV confirming the existence of a collective plasma resonance.

4. Conclusion

In summary, we have explored the electronic and optical properties of Cd-doped ZnO NS using all electrons full-potential linearized augmented plane wave (FP-LAPW) method based on DFT within generalize gradient approximation (GGA). The calculated electronic band structure have shown that Cd-doped ZnO NS exhibited a direct band gap of 1.5 eV compared to 1.7 eV of the pure ZnO NS. The changes in the band gap have affected automatically the optical properties, that we investigated with purpose to examine their potential impact in various applications. The reduction of the band gap due to the Cd doping and the possibility of blue-white fluorophore transition, have made feasible the use of Cd-doped ZnO NS for light-emitting devices and PV applications.

Author details

Saleem Ayaz Khan[1]
E-mail: saleemayaz_hu@yahoo.com
Sikander Azam[2]
E-mail: sikander.physicst@gmail.com
Mohammed Benali Kanoun[3]
E-mail: mkanoun@alfaisal.edu
Ghulam Murtaza[4]
E-mail: murtaza@icp.edu.pk
Malika Rani[5]
E-mail: wirdeali14@yahoo.com
Souraya Goumri-Said[3]
E-mail: sosaid@alfaisal.edu
ORCID ID: http://orcid.org/0000-0002-9333-7862

[1] New Technologies–Research Centre, University of West Bohemia, Univerzitni 8, 306 14 Pilsen, Czech Republic.
[2] Department of Physics, The University of Lahore, Sargodha Campus, 40100 Pilsen, Pakistan.
[3] Department of Physics, College of Science, Alfaisal University, P.O. Box 50927, Riyadh 11533, Saudi Arabia.
[4] Materials Modeling Lab, Department of Physics, Islamia College University, Peshawar, Pakistan.
[5] Department of Physics, The Women University Multan, Multan, Pakistan.

Citation information

Cite this article as: Tailoring the electronic structure and optical properties of cadmium-doped zinc oxides nanosheet, Saleem Ayaz Khan, Sikander Azam, Mohammed Benali Kanoun, Ghulam Murtaza, Malika Rani & Souraya Goumri-Said, *Cogent Physics* (2017), 4: 1391734.

References

Al-Sunaidi, A., & Goumri-Said, S. (2011). Investigating the adsorption of H2O on ZnO nanoclusters by first principle calculations. *Chemical Physics Letters, 507*(1–3), 111–116. https://doi.org/10.1016/j.cplett.2011.03.041

Avouris, P., Chen, Z., & Perebeinos, V. (2007). Carbon based electronics. *Nature Nanotechnology, 2*, 605–615. https://doi.org/10.1038/nnano.2007.300

Bantounas, I., Goumri-Said, S., Benali Kanoun, M. B., Manchon, A., Roqan, I., & Schwingenschlögl, U. (2011). Ab initio investigation on the magnetic ordering in Gd doped ZnO. *Journal of Applied Physics, 109*(8), 083929. https://doi.org/10.1063/1.3574924

Blaha, P., Schwarz, K., Madsen, G. K. H., Kvasnicka, D., & Luitz, J. (2008). *An augmented plane wave plus local orbitals program for calculating crystal properties, WIEN2 K*. Vienna: Austria.

Claeyssens (2005). Growth of ZnO thin films experiment theory. *Journal of Materials Chemistry, 15*(1), 139–148. https://doi.org/10.1039/B414111C

Delin, A., Ravindran, P., Eriksson, O., & Wills, J. M. (1998). Full potential optical calculations of lead chalcogenides. *International Journal of Quantum Chemistry, 69*, 349–358. https://doi.org/10.1002/(ISSN)1097-461X

Duan, J., Huang, X., & Wang, E. (2005). PEG-assisted synthesis of ZnO nanotubes. *Materials Letters, 60*, 1918–1921.

Fiorentini, V., & Baldereschi, A. (1995). Dielectric scaling of the self energy scissor operator in semiconductors insulators. *Physical Review B, 51*(23), 17196–17198. https://doi.org/10.1103/PhysRevB.51.17196

Geim, A., & Novoselov, K. (2007). The rise of graphene. *Nature Materials, 6*(3), 183–191. https://doi.org/10.1038/nmat1849

Hohenberg, P., & Kohn, W. (1964). Inhomogeneous electron gas. *Physical Review, 136*(3B), B864–B871. https://doi.org/10.1103/PhysRev.136.B864

Huang, Y., He, J., Zhang, Y., Dai, Y., Gu, Y., Wang, S., & Zhou, C. (2006). Morphology structures properties of ZnO nanobelts fabricated by Zn powder evaporation without catalyst at lower temperature. *Journal of Materials Science, 41*(10), 3057–3062. https://doi.org/10.1007/s10853-006-6978-9

Hwang, D.-K., Oh, M.-S., Lim, J., & Park, S.-J. (2007). ZnO thin films light emitting diodes. *Journal of Physics D: Applied Physics, 40*(22), R387–R412. https://doi.org/10.1088/0022-3727/40/22/R01

Kanoun, M. B., Goumri-Said, S., Manchon, A., & Schwingenschlögl, U. (2015). Ferromagnetism carried by highly delocalized hybrid states in Sc-doped ZnO thin films. *Applied Physics Letters, 100*(22), 222406.

Katsnelson, M. I., Novoselov, K. S., & Geim, A. K. (2006). Chiral tunnelling the Klein paradox in graphene. *Nature Physics, 2*, 620–625. https://doi.org/10.1038/nphys384

Khan, S. A., Azam, S., Shah, F. A., Amin, B. (2015). Electronic structure and optical properties of CdO from bulk to nanosheet: DFT approach. *Optical Materials, 47*, 372–378. https://doi.org/10.1016/j.optmat.2015.06.007

Kittel, C. (1996). *Introduction to solid state physics*. New York City, NY: Wiley. ISBN 0-471-14286-7.

Kulkarni, A. J., Zhou, M., Sarasamak, K., & Limpijumnong, S. (2006). Novel phase transformation in ZnO nanowires under tensile loading. *Physical Review Letters, 97*(10), 105502.

Law, M., Greene, L. E., Johnson, J. C., Saykally, R., & Yang, P. (2005). Nanowire dye sensitized solar cells. *Nature Materials, 4*(6), 455–459. https://doi.org/10.1038/nmat1387

Lin, Y., & Connell, J. W. (2012). Advances in 2D boron nitride nanostructures nanosheets nanoribbons nanomeshes hybrids with graphene. *Nanoscale, 4*, 6908–6939. https://doi.org/10.1039/c2nr32201c

Ma, K. L., Yan, X. H., Xiao, Y., & Chen, Y. P. (2010). Electronic transport properties of metallic graphene nanoribbons with two vacancies. *Solid State Communications, 150*(29–30), 1308–1312. https://doi.org/10.1016/j.ssc.2010.05.011

Novoselov, K. S., Geim, A. K., Morozov, S. V., Jiang, D., Katsnelson, M. I., Grigorieva, I. V., ... Firsov, A. A. (2005). Two dimensional gas of massless Dirac fermions in graphene. *Nature, 438*(7065), 197–200. https://doi.org/10.1038/nature04233

Ouyang, F., Peng, S., Liu, Z., & Liu, Z. (2011). B gap opening in graphene antidot lattices the missing half. *ACS Nano, 50*, 4023–4030. https://doi.org/10.1021/nn200580w

Penn, D. R. (1960). Wave-number-dependent dielectric function of semiconductors. *Physical Review, 128*, 2093.

Perdew, J. P., Burke, K., & Ernzerhof, M. (1996). Generalized gradient approximation made simple. *Physical Review Letters, 77*(18), 3865–3868. https://doi.org/10.1103/PhysRevLett.77.3865

Ul Haq, B., Ahmed, R., & Goumri-Said, S. (2014). DFT characterization of cadmium doped zinc oxide for photovoltaic solar cell applications. *Solar Energy Materials and Solar Cells, 130*, 6–14. https://doi.org/10.1016/j.solmat.2014.06.014

Vempati, S., Mitra, J., & Dawson, P. (2012). One step synthesis of ZnO nanosheets a blue white fluorophore. *Nanoscale Research Letters, 7*(1), 470. https://doi.org/10.1186/1556-276X-7-470

Wang, Q., Sun, Q., Chen, G., Kawazoe, Y., & Jena, P. (2008). Vacancy induced magnetism in ZnO thin films nanowires. *Physical Review B, 77*, 15019. https://doi.org/10.1103/PhysRevB.77.205411

Wang, Y., Fan, X., & Sun, J. (2009). Hydrothermal synthesis of phosphate mediated ZnO nanosheets. *Materials Letters, 63*(3–4), 350–352. https://doi.org/10.1016/j.matlet.2008.10.036

Zhang, J., Zhao, S.-Q., Zhang, K., Zhou, J.-Q., & Cai, Y.-F. (2012). A study of photoluminescence properties performance improvement of Cd doped ZnO quantum dots prepared by the sol gel method. *Nanoscale Research Letters, 7*(1), 405. https://doi.org/10.1186/1556-276X-7-405

Cogent Physics (ISSN: 2331-1940) is published by Cogent OA, part of Taylor & Francis Group.

Publishing with Cogent OA ensures:

- Immediate, universal access to your article on publication
- High visibility and discoverability via the Cogent OA website as well as Taylor & Francis Online
- Download and citation statistics for your article
- Rapid online publication
- Input from, and dialog with, expert editors and editorial boards
- Retention of full copyright of your article
- Guaranteed legacy preservation of your article
- Discounts and waivers for authors in developing regions

Submit your manuscript to a Cogent OA journal at www.CogentOA.com